applied sciences

MDPI

Article

Predicting Wear Rate and Friction Coefficient of $Li_2Si_2O_5$ Dental Ceramic Using Optimized Artificial Neural Networks

Marko Pantić [1], Saša Jovanović [2], Aleksandar Djordjevic [2,*], Suzana Petrović Savić [2], Milan Radenković [1] and Živče Šarkoćević [1]

[1] Department of Production Engineering, Faculty of Technical Sciences, University of Priština in Kosovska Mitrovica, 38220 Kosovska Mitrovica, Serbia; marko.pantic@pr.ac.rs (M.P.); milan.radenkovic@pr.ac.rs (M.R.); zivce.sarkocevic@pr.ac.rs (Ž.Š.)

[2] Faculty of Engineering, University of Kragujevac, 34000 Kragujevac, Serbia; dviks@kg.ac.rs (S.J.); petrovic.suzana@gmail.com (S.P.S.)

* Correspondence: adjordjevic@kg.ac.rs

Abstract: The tribological properties of dental materials, such as wear and friction, are crucial for ensuring their long-term reliability and performance. Traditional experimental approaches, while accurate, are often resource intensive and time consuming, prompting a need for efficient computational methods. This study explores the application of artificial neural networks (ANNs) to predict the tribological behavior of dental ceramic lithium disilicate (IPS e.max Cad). A genetic algorithm (GA) was used to optimize the ANN's hyperparameters, improving its ability to model complex, nonlinear relationships between input variables, including normal load and velocity and output properties such as wear rate and friction coefficients. By integrating experimental data with an ANN, this study identifies key factors influencing tribological performance, reducing the dependency on extensive experimental testing. The results demonstrate that the optimized ANN model accurately predicts tribological behavior, offering a robust framework for material optimization. These findings emphasize the potential of combining ANNs and GAs to enhance the understanding and design of dental materials, accelerating innovation while addressing the challenges of traditional evaluation methods. This research underscores the transformative role of advanced computational approaches in tribology and material science.

Keywords: prediction models; computer neural network; dental wear; friction; lithium disilicate

Academic Editor: Vittorio Checchi

Received: 22 December 2024
Revised: 4 February 2025
Accepted: 7 February 2025
Published: 10 February 2025

Citation: Pantić, M.; Jovanović, S.; Djordjevic, A.; Petrović Savić, S.; Radenković, M.; Šarkoćević, Ž. Predicting Wear Rate and Friction Coefficient of $Li_2Si_2O_5$ Dental Ceramic Using Optimized Artificial Neural Networks. *Appl. Sci.* **2025**, *15*, 1789. https://doi.org/10.3390/app15041789

1. Introduction

The study of tribological properties—friction, wear, and lubrication—is essential for understanding material performance in applications where mechanical contact is a critical factor. These properties directly influence the reliability, efficiency, and longevity of components in industries such as automotive, aerospace, and biomedical engineering [1]. Traditional methods for evaluating tribological properties rely primarily on experimental testing, which, while accurate, can be resource intensive, time consuming, and sometimes inconsistent due to environmental variability [2,3]. Some of the most widely used techniques include pin-on-disk testing, which involves a stationary pin loaded against a rotating disk, allowing researchers to analyze the wear rate and friction coefficient under controlled conditions. However, this method may not fully replicate real-world dynamic interactions between materials. Reciprocating tribometers is used to simulate an oscillatory sliding motion, which is particularly relevant in dental applications where mastication induces cyclic contact between surfaces. Micro- and nanoindentation are used to measure hardness,

elasticity, and wear resistance at micro- and nanoscale levels. While highly precise, they may not provide comprehensive tribological insights for bulk material behavior; Scanning Electron Microscopy (SEM) and Atomic Force Microscopy (AFM) are essential for examining worn surfaces, detecting surface roughness, and identifying wear mechanisms such as adhesion, abrasion, and fatigue wear. However, these methods are post-mortem analyses, meaning they do not allow for the real-time observation of wear progression [2,4,5]. Despite their precision, these traditional approaches face significant limitations. They often require extensive testing cycles, costly instrumentation, and complex data interpretation. Additionally, they may not adequately capture the multifactorial and nonlinear interactions between material composition, contact pressure, sliding velocity, and environmental conditions, all of which influence wear and friction behavior [1].

To overcome the limitations of traditional experimental methods, researchers have increasingly turned to computational and artificial-intelligence-based models to enhance material characterization. These approaches reduce testing time, improve predictive accuracy, and optimize material selection processes in tribology research. Among these methods, artificial neural networks (ANNs) have gained prominence due to their ability to model complex, nonlinear relationships between input parameters (e.g., load, velocity, and material composition) and tribological properties (e.g., wear rate and friction coefficient). Their adaptability and capacity to process large datasets have led to their widespread adoption in materials science, where they facilitate predictive modeling, the optimization of material properties, and a reduced need for exhaustive experimental studies. The application of ANNs in tribological research spans multiple domains, including composite materials, polymer-based systems, and biomedical applications. In composite materials, ANN models have been successfully used to predict wear and friction behavior in fiber-reinforced composites by incorporating variables such as fiber orientation, applied load, and sliding velocity, demonstrating high accuracy in capturing complex material interactions [6]. Similarly, ANNs have shown potential in optimizing surface treatment techniques, such as plasma nitriding, where predictive models estimate wear resistance based on process parameters like treatment temperature and duration [7]. In polymer-based tribological systems, ANNs have proven effective in modeling the wear behavior of polymer composites, including carbon-fiber-reinforced materials. By analyzing key tribological parameters such as contact pressure, temperature, and mechanical load, ANN-based models have successfully predicted wear loss and friction coefficients with remarkable precision [8,9]. Additionally, studies on polyphenylene sulfide (PPS) composites have demonstrated that optimizing ANN architectures and learning parameters improves predictive accuracy and ensures robustness across various testing conditions [10]. While other machine learning (ML) techniques, such as k-nearest neighbors (KNN) and gradient boosting algorithms like XGBoost, have been successfully applied to similar studies, ANNs remain underutilized for predicting the tribological characteristics of dental ceramics. Given the complexity of interactions between the ceramic microstructure, mechanical loading, and wear mechanisms, ANNs present a promising tool for capturing nonlinear dependencies that traditional statistical models may overlook. Recent studies have started employing ANNs in a tribological analysis of advanced coatings, reinforcing the potential of these models for predicting material behavior under different operating conditions [11].

Despite the widespread application of ANNs in tribology, its use in dental material research remains relatively limited. While ML techniques have been employed in predicting the mechanical properties of dental composites, such as tensile strength and bond durability, the modeling of tribological behavior, including wear resistance and friction coefficients, has not been extensively investigated. Some studies have explored the use of ANNs in dental applications, such as predicting the mechanical performance of adhesives

and composite formulations [12]. Recent research has also applied ANN models to assess wear behavior in dental composites, demonstrating their potential in identifying the key material and environmental factors that influence tribological properties [13]. This study aims to bridge this research gap by utilizing ANNs to model and predict the tribological performance of lithium disilicate dental ceramics under various testing conditions, ultimately contributing to the advancement of computational intelligence in dental tribology. In recent decades, advancements in dental materials have revolutionized dentistry, particularly with the introduction of metal-free ceramics. These materials combine durability and aesthetics, enabling restorations that closely mimic natural teeth. Modern ceramic systems offer exceptional strength and aesthetics, making them essential in contemporary practice. Among these, lithium disilicate ceramics stand out for their superior properties, redefining the standards of modern dentistry. Lithium disilicate ceramics have become the gold standard in metal-free dental restorations due to their superior aesthetic and mechanical properties. This material is characterized by a high crystal content (~70%), which provides exceptional flexural strength and wear resistance, making it ideal for crowns, inlays, onlays, and veneers [14]. In the past decade, research has focused on optimizing the microstructure of lithium disilicate ceramics. High-Density Micronization (HDM) technology enables uniform crystal dispersion, resulting in enhanced fracture resistance and aesthetics [15]. Additionally, innovative manufacturing techniques, such as 3D printing [16], have gained attention for their potential to improve ceramic processing and material performance, further expanding the possibilities for dental applications. This technology allows for flexural strength up to 500 MPa, with minimal risk of wear to opposing teeth [17].

Based on previous research and the identified research gap, this study tests the null hypothesis that there is a significant correlation between experimental parameters, such as normal load and the sliding velocity, and the predicted values of the wear rate and friction coefficient using ANNs. Additionally, it examines whether ANN models optimized with a genetic algorithm (GA) manage to improve the prediction accuracy compared to traditional methods for analyzing tribological data. These hypotheses will be evaluated through a combination of experimental investigations and computational simulations, with their validity assessed based on the obtained results.

This paper seeks to build on the growing body of research into the use of ANNs for predicting tribological properties (the wear rate and friction coefficient) of commercial dental ceramic lithium disilicate (IPS e.max Cad). This study aims to assess the efficacy of ANNs in capturing the complex, nonlinear relationships that govern material behavior under friction and wear. The following sections detail the methodology employed, present the results obtained, and discuss their implications within the broader context of tribology and material science. Ultimately, this research underscores the transformative potential of ANNs as a tool for material optimization and innovation in tribological studies.

2. The Materials and Methods

2.1. Material and Sample Preparation

The first significant advancements in the development of all-ceramic systems were achieved by Ivoclar Vivadent AG from Liechtenstein with the introduction of the IPS Empress system in 1991. The commercial material IPS e.max CAD is a lithium disilicate ceramic designed for use in CAD/CAM systems, characterized by its high flexural strength and wide applicability in the fabrication of restorations and dental bridges. CAD/CAM blocks are blue, monolithic, and exist in the metasilicate phase (partially crystallized, Li_2SiO_3). In their raw state, these blocks exhibit low flexural strength, which facilitates efficient processing within CAD/CAM systems. Through a crystallization process, the final lithium disilicate crystal structure ($Li_2Si_2O_5$) is formed, resulting in a significantly

increased flexural strength of 360 MPa. IPS e.max CAD is a fully ceramic material renowned for its high aesthetic quality, making it well suited for prosthetic applications as it fulfills essential requirements for aesthetics, functionality, and material biocompatibility [4]. The chemical composition of IPS e.max CAD includes the following proportions: 57–80 wt.% SiO_2, 11–19 wt.% Li_2O, 0–13 wt.% K_2O, 0–11 wt.% P_2O_5, 0–8 wt.% ZrO_2, 0–8 wt.% ZnO, 0–5 wt.% Al_2O_3, and 0–5 wt.% MgO [18].

All samples have a block shape, with dimensions of 18 mm in length, 14 mm in width, and 12 mm in height. The contact surfaces of the samples were prepared using three different finishing techniques: polishing, glazing, and grinding. The first sample underwent polishing on a polishing machine with controlled speed, using diamond sandpaper of varying grit sizes (280, 400, 600, 800, 1200, and 2000) under hand-applied pressure and water cooling. Fine polishing was subsequently performed with liquid emulsions containing particles of 6 µm and 0.04 µm grain size (DP suspension and O-M In Suspension). The second sample's contact surface was glazed in accordance with the manufacturer's instructions, involving vacuum treatment at an entry temperature of 400 °C and a peak temperature of 730 °C for 1 min [18,19]. Lastly, the third sample's contact surface was ground using a diamond bur (Medin, ISO: 806 314 146 534 016, 150 µm—max [20]). The grinding process was performed manually, with the sample loosely fixed, resulting in variable pressure applied to the surface depending on hand movement. The goal of different finishing techniques is to simulate the actual contact conditions of the finishing treatments for aesthetic restorations, which are inevitable in practice.

2.2. AFM Analysis

All results of 3D surface topography and roughness parameters were obtained by AFM of NT-MDT (Moscow, Russia) manufacturers.

For this experiment, contact mode was used at room temperature, with the tip of the AFM cantilever (a radius of 10 nm) remaining in constant contact with the lithium disilicate sample surface. The software continuously monitors and records the bending and/or twisting of the cantilever due to surface roughness variations and captures all the results [4]. In this way, highly precise 3D surface topographies of the different prepared samples are reconstructed. The measurement area for all samples was 100 × 100 µm.

Before all tests, to remove residual contaminants, the surfaces were cleaned with 70% alcohol using a soft cotton cloth, followed by ultrasonic cleaning in distilled water for 30 min. The samples were then air dried at room temperature.

2.3. Tribological Test

Tribological tests in vitro were realized using a ball-on-flat configuration with the CSM nanotribometer, employing a linear reciprocating module (Figure 1a) in an artificial saliva medium. A commercial alumina ball (Al_2O_3) with a diameter of 1.5 mm was used as the stationary contact body (Figure 1b). Alumina is known for its ultra-high hardness (9 on the Mohs scale [21], just below diamond) and excellent wear resistance. All the tests were repeated three times, and the reproducibility of the tribological behavior was fairly confirmed. The characteristics of the conducted tribological tests are given in Table 1.

The tribological tests were conducted in the presence of artificial saliva to simulate more realistic conditions of the oral environment. This setup is based on findings from previous studies [22], which demonstrated that artificial saliva could act as a coolant and lubricant during wear processes. Additionally, the presence of artificial saliva was shown to reduce the risk of damage to the contact surfaces of materials when compared to dry conditions. The lubrication mechanism in this case is facilitated by the complete separation of sliding surfaces by a thin layer of saliva [23].

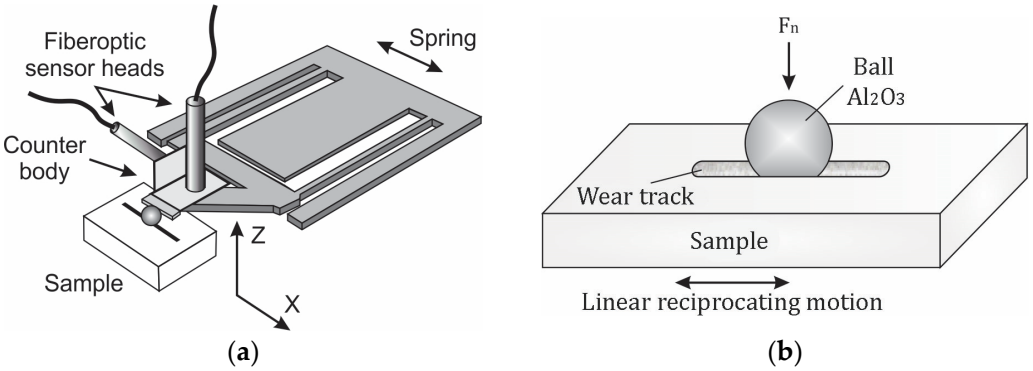

Figure 1. (**a**) Linear reciprocating module; (**b**) contact geometry [4].

Table 1. Tribological input parameters.

Instrument Preferences
Linear reciprocating module (linear mode acquisition) Half of amplitude: 0.5 mm Frequency: 100 Hz Ambient air temperature: 23 ± 2 °C
Tested samples
Commercial lithium disilicate—IPS e.max CAD (Ivoclar Vivadent, Schaan, Liechtenstein) Finishing procedures of samples: polishing, glazing, and grinding
Static body
Commercially supplied ball: alumina (Al_2O_3) Ball diameter: 1.5 mm
Normal load values
Fn: 250 mN; 500 mN; 750 mN; 1000 mN
Maximum linear velocity values
v: 4 mm/s; 8 mm/s; 12 mm/s
The test duration
10,000 cycles (20 m)
Environment contact zone
Artificial saliva medium

The tribological tests were aimed at tracking the wear and friction values as a function of the sliding distance. The coefficient of friction values was recorded in real time during the tests using TRIBOX 2.9.0 software. After each test, the samples were removed from the nanotribometer, and the wear tracks were documented using an Optical Microscope (MEIJI Techno, Tokyo, Japan) and Scanning Electron Microscope (JEOL JSM-6610 LV, Tokyo, Japan).

After each completed test, the wear volume of the samples was determined based on the measured width and length of the wear tracks, as measured through Optical Microscopy and the software Infinity Analyze, version number: 6.5.0, according to ASTM G133-05 [24,25]. The wear volume (V) was calculated using the measured wear track length and its average cross-sectional area. The cross-sectional area was assumed to be a flat segment of a sphere corresponding to the geometry of the Al_2O_3 ball. Measurements were taken at three equally spaced locations along the wear track to ensure uniformity, as required by the standard. Given that the wear of the alumina ball can be characterized as 'unmeasurable wear', only the wear of the flat sample was measured and

calculated. The wear rate (W), representing the material removal per unit sliding distance, was calculated using the following equation [26]:

$$W = V/s, [mm^3/m], \quad (1)$$

where:

V—is the wear volume of the material [mm^3].

s—is the sliding distance [m].

The total sliding distance of 20 m was used for the calculations. The wear rate was calculated for each test to quantify the material's wear performance.

2.4. Machine Learning Model Setup

To predict the tribological properties of lithium disilicate, an ANN model was employed. The structure of the ANN was optimized using a GA, which was used to determine the optimal architecture for the network, including the number of layers, number of neurons per layer, and activation functions. The GA ensures that the network structure is highly adapted to the specific problem, allowing for the accurate prediction of wear and friction properties based on various input variables, such as material composition, filler content, and operational conditions.

The ANN was trained on a dataset containing both experimental data and data sourced from the relevant literature. Input features for the model included material composition, processing conditions, normal load, and linear velocity, while the output properties were the wear rate and friction coefficient. The model was implemented using MatLab2017, and the GA was used to fine-tune the model parameters. The following pseudo code provides a clear overview of the entire process of training and optimizing an artificial ANN using a GA (Table 2).

In this study, an ANN was used to model the relationship between tribological parameters (normal force and sliding velocity) and the resulting wear rate and coefficient of friction. ANNs were chosen due to their ability to approximate complex functions and generalize relationships between input and output data. The structure of the used ANN model is three-layered: an input layer, one hidden layer, and an output layer. The input layer consists of two neurons corresponding to the tribological parameters (normal force, F_n, and velocity, v) while the output layer has one neuron for predicting the wear rate (W) or coefficient of friction (COF).

To optimize the parameters of the ANN model, such as the number of neurons in the hidden layer, type of transfer function for the hidden and output layer, number of epochs, etc., a GA was applied. The GA is a method based on natural selection and evolution, which is used for searching large and complex parameter spaces to find the optimal set of parameters for the ANN. The GA was applied to optimize the ANN structure with the objective function to minimize the error function (MSE), thereby improving the model's performance. This approach allows for better generalization of the ANN model, reducing issues like overtraining and overfitting. The parameters being optimized include the number of hidden neurons, transfer function for the hidden layer, transfer function for the output layer, training validation test data split ratio, training coefficient, number of epochs, and training function. For the optimization of these parameters, the lower and upper bounds were applied as defined in Table 3.

The performance of the ANN models was evaluated using the MSE for each subset (training, validation, and testing). The models that best predict the wear rate and coefficient of friction under different surface conditions were selected based on these criteria.

Table 2. Pseudo code for ANN training and GA optimization.

1. Load and Preprocess Data:
   - Load the dataset and split into training and testing sets.
   - Preprocess data (normalization, missing values handling, etc.).
2. Define the Neural Network Architecture:
   - Define the network structure (e.g., number of layers, number of neurons).
   - Define the transfer functions for the hidden and output layers.
   - Initialize the ANN with specified configurations.
3. Set Up Genetic Algorithm Parameters:
   - Define the number of generations, population size, mutation rate, etc.
   - Set the bounds for each parameter to be optimized (e.g., number of neurons, transfer functions, training ratio).
   - Define the fitness function, which evaluates the error between the network's predictions and the true outputs (e.g., mean squared error).
4. Optimization Process with Genetic Algorithm:
   - Start the genetic algorithm loop:
   - Generate an initial population of candidate ANN configurations.
   - Evaluate the fitness of each candidate by training the ANN on the training data and calculating its error on the validation set.
   - Select individuals based on their fitness (tournament selection or roulette wheel selection).
   - Apply crossover and mutation operators to create new generations.
   - Repeat for a specified number of generations or until convergence is achieved.
5. Train the Best ANN:
   - Train the selected best ANN configuration with the full training data.
   - Use early stopping to avoid overfitting.
6. Evaluate the Trained Model:
   - Evaluate the performance of the trained model on both the training and testing datasets.
   - Calculate performance metrics (e.g., MSE, accuracy).
7. Save the Results:
   - Save the optimized ANN model and the training logs.
   - Return the trained ANN model for future use.

Table 3. Boundary conditions for neural network optimization with genetic algorithm.

Hyperparameter	Description	Lower Bound	Upper Bound	Specific Function Used
Number of hidden neurons	Number of neurons in the hidden layer	15	40	N/A
Transfer function for the hidden layer	Type of activation function for the hidden layer	1	Number of available transfer functions	Elliott Sigmoid Transfer Function, Logarithmic Sigmoid Transfer Function, Softmax Transfer Function
Transfer function for the output layer	Type of activation function for the output layer	1	Number of available transfer functions	Elliott Sigmoid Transfer Function, Logarithmic Sigmoid Transfer Function, Softmax Transfer Function
Training validation test ratio	Proportion of data split between training, validation, and testing	0	0.25	N/A
Training coefficient (mc)	Coefficient controlling the learning rate or momentum	0.1	0.9	N/A
Number of epochs (epochs)	Maximum number of training iterations	50	2000	N/A
Training function	Type of training algorithm used	1	Number of available training functions	BFGS Quasi-Newton Backpropagation, Conjugate Gradient with Powell–Beale Restarts, Fletcher–Reeves Conjugate Gradient, Polak–Ribiére Conjugate Gradient, Gradient Descent with Adaptive Learning Rate, Gradient Descent with Momentum, Gradient Descent with Momentum and Adaptive Learning Rate, Levenberg–Marquardt Backpropagation, One Step Secant Backpropagation, Resilient Backpropagation.

3. Results

3.1. AFM Results

Figures 2–4 present the AFM analysis of 3D topographies and roughness profiles of all samples, obtained under different finishing techniques before the tribological tests. The surface roughness of each sample was measured along the same reference length (vertically), as shown in the 2D views of Figures 2a, 3a and 4a.

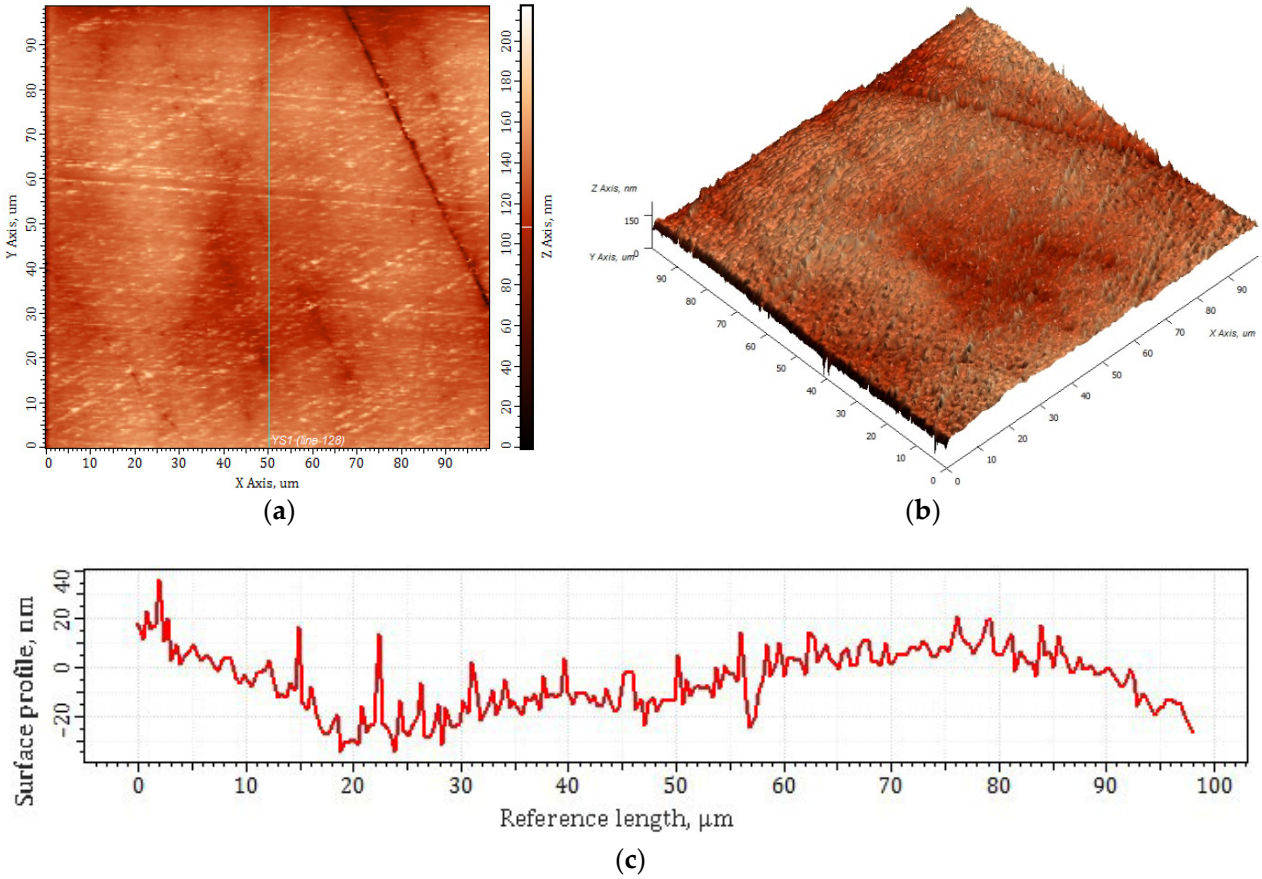

Figure 2. AFM analysis of the polished surface of commercial lithium disilicate ceramic (IPS e.max CAD): (**a**) 2D representation of the reference length; (**b**) 3D topography; (**c**) surface profile.

Also, the previously presented AFM 3D topographies were verified through the selected roughness parameter values, which are presented in Table 4.

Table 4. Roughness parameters under different finishing techniques of commercial lithium disilicate ceramic (IPS e.max Cad).

Measurement Range, 100 × 100 µm	Roughness Parameters			
	Ra	Rz	Rmax	Rq
Polished surface	9.595 nm	46.923 nm	66.575 nm	12.281 nm
Glazed surface	19.817 nm	68.454 nm	147.965 nm	25.108 nm
Ground surface	0.686 µm	2.123 µm	4.186 µm	0.854 µm

The presented roughness parameters (Ra, Rz, Rmax, and Rq) for each sample were measured along the same vertical reference length, and their values were automatically obtained and read from the AFM software (Version: Nova PX) after the completion of each single measurement.

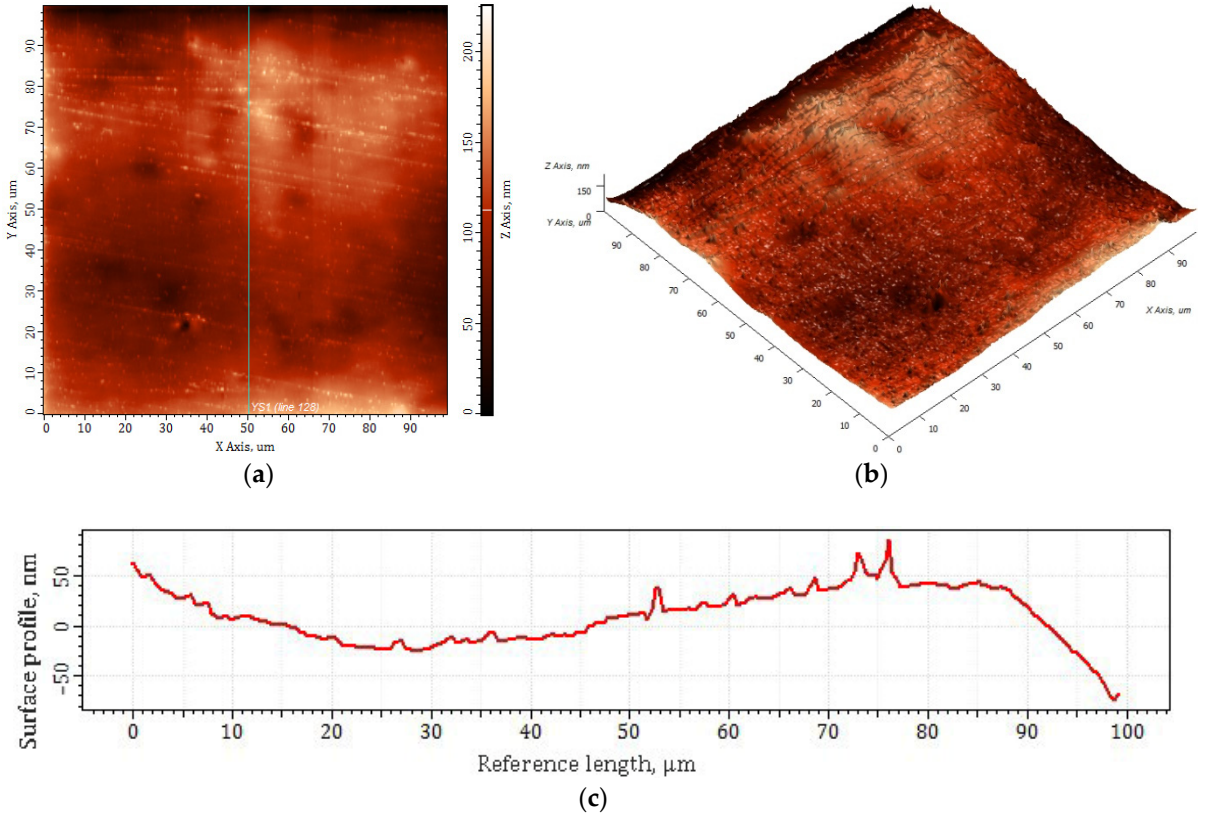

Figure 3. AFM analysis of the glazed surface of commercial lithium disilicate ceramic (IPS e.max Cad): (**a**) 2D representation of the reference length; (**b**) 3D topography; (**c**) surface profile.

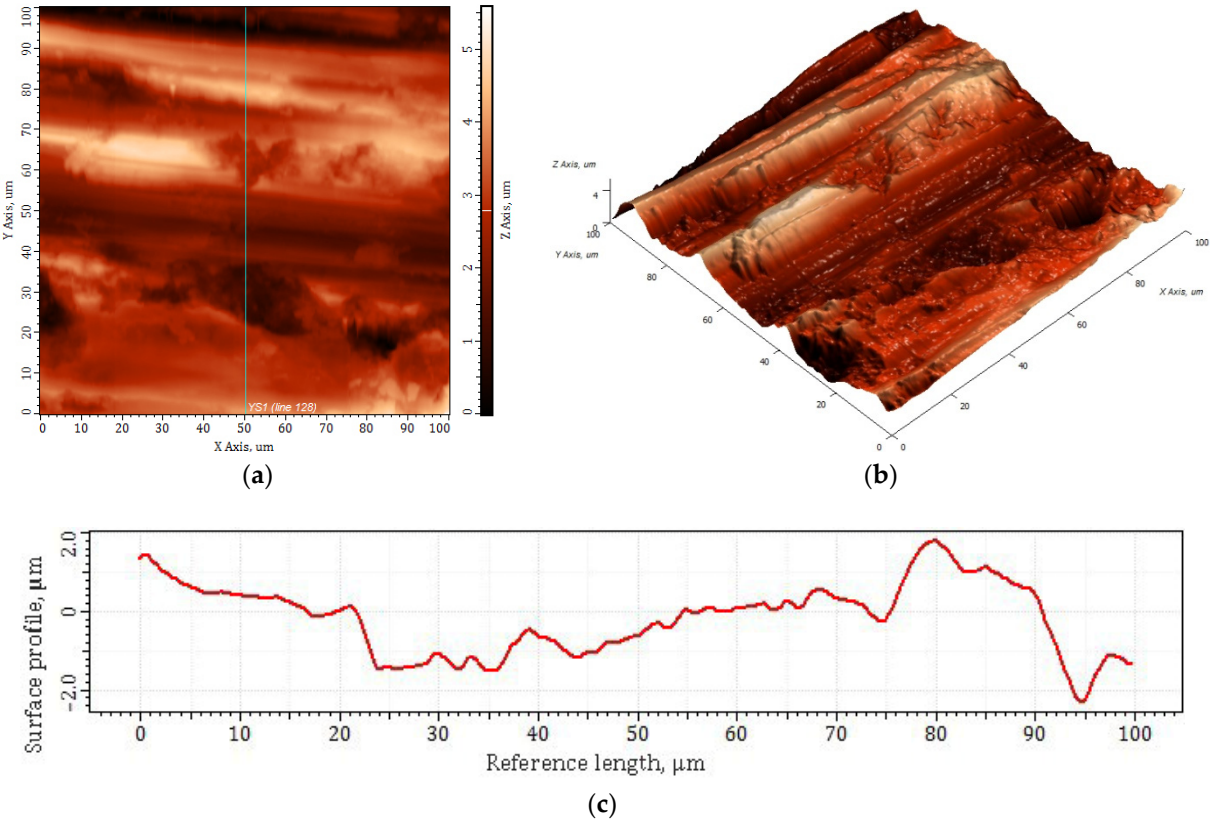

Figure 4. AFM analysis of the ground surface of commercial lithium disilicate ceramic (IPS e.max Cad): (**a**) 2D representation of the reference length, µm; (**b**) 3D topography; (**c**) surface profile.

The presented surface roughness results of all finishing techniques are of great importance for the analysis of tribological characteristics in the initial moments of contact when the microgeometry of the contact surfaces plays a very significant role in tribological phenomena, friction, and wear.

3.2. Tribological Results

The analysis of wear tracks was conducted using Optical Microscopy (OM) and Scanning Electron Microscopy (SEM). As a representative example, Figure 5 presents OM (left) and SEM (right) micrographs of wear tracks on IPS e.max CAD samples prepared with different finishing techniques. The tribological tests were performed in an artificial saliva medium under a load of 1 N, a sliding velocity of 8 mm/s, and 10,000 fretting cycles. The results indicate that abrasive wear is the predominant wear mechanism.

Within the wear tracks, deformation and damage of the smooth contact surface are evident in the form of tribo layers formation and the appearance of numerous micro cracks. As the sliding velocity increases due to the linear reciprocating motion, existing cracks gradually propagate over time. The delamination of tribo layers, caused by the constant sliding of the ball, leads to the fragmentation of wear debris, ultimately resulting in three-body abrasion. The process of material removal and the formation of new tribo layers is continuous and persists throughout the duration of the test.

Wear tracks in the cases of 250 mN, 500 mN, and 750 mN were similar to the exhibited one for 1 N. However, with the increase in normal load (Fn), the wear track width visibly increased for all tested surfaces. Based on the aforementioned statements, the mathematically obtained wear rate (W) results for all finishing procedures demonstrated a trend of increasing wear rate with the rise in normal load and sliding velocity.

Figure 6 presents a representative example of the coefficient of friction (COF) diagram for the polished contact surface of the commercial lithium disilicate material (IPS e.max CAD) under two selected testing conditions (F_1V_1 = 250 mN, 4 mm/s, and F_4V_3 = 1000 mN, 12 mm/s) over a duration of 10,000 cycles with the presence of artificial saliva in the contact zone.

In the presented diagram (Figure 6), it is clearly observed that the COF decreases with increasing normal load. Generally, COF values declined with increasing force across all conducted tests of different surface techniques on the nanotribometer. The distribution and occurrence of peaks in the COF curve can serve as important indicators of various influences and changes in wear mechanisms during testing. The frictional behavior of the examined material surfaces varies depending on the different surface techniques.

In general, the ground surface finish exhibited the best frictional properties under various testing conditions, which included three sliding velocities and four load levels. The COF values of the ground surface directly correlate with the wear rate for the same surface. This is due to the nature of contact formation, as the reciprocating linear motion of the Al_2O_3 ball on the ground sample's contact surface occurs exclusively on the asperity peaks, which vary in height. As a result, the presence of wear debris in the contact zone is minimal, as the reciprocating linear motion facilitates its removal through numerous channels (grinding scars) formed by the valleys between asperities, aided by the artificial saliva flow. This phenomenon is clearly illustrated in the SEM image of the ground surface (Figure 5). Consequently, the influence of the "third body" effect on the COF values is minimized, unlike in polished and glazed surface finishes.

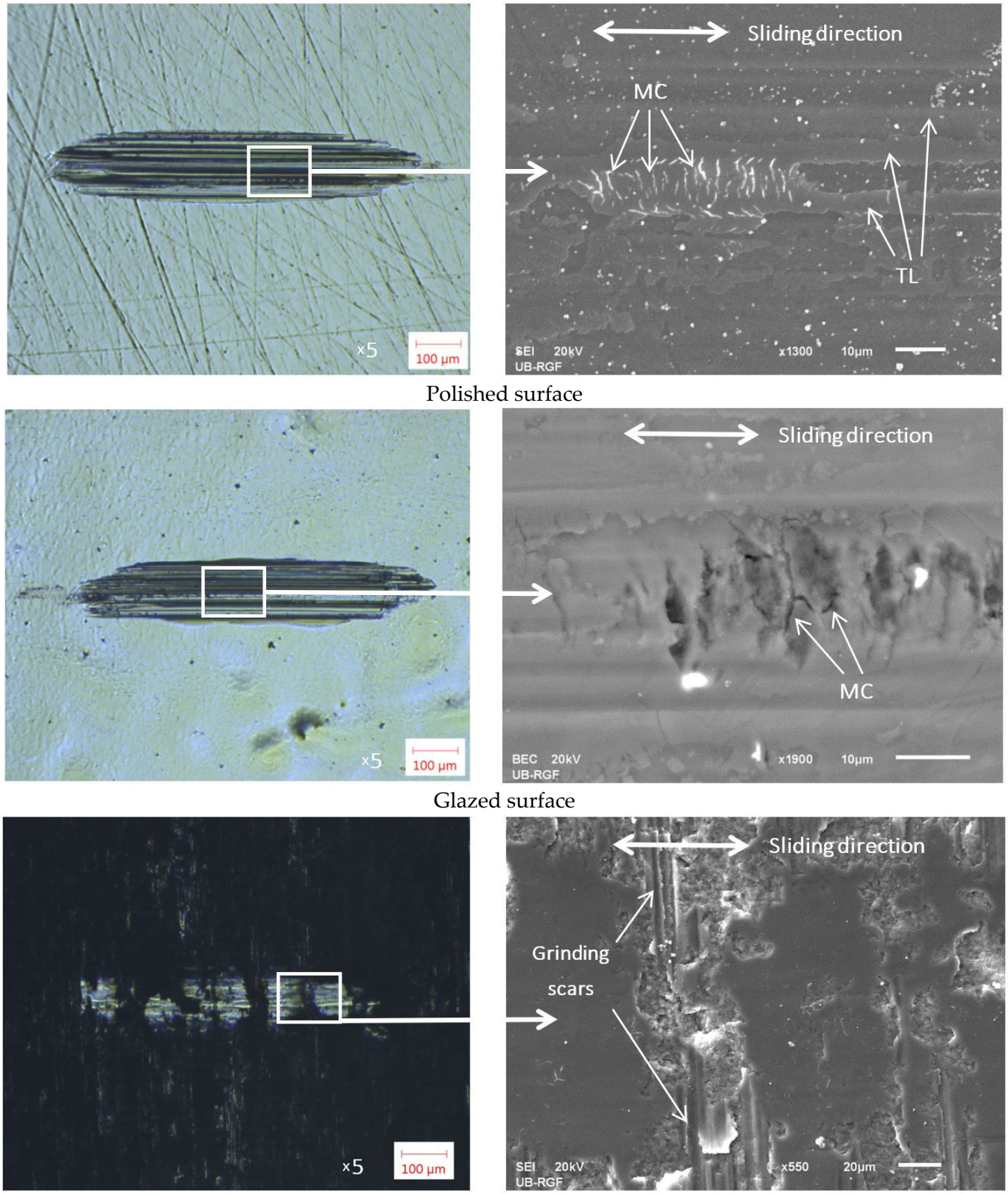

Figure 5. OM (**left**) and SEM (**right**) micrographs of wear tracks on IPS e.max CAD samples (under different finishing techniques) in the presence of artificial saliva, Fn = 1 N, v = 8 mm/s, and 10,000 fretting cycles. (MC—micro cracks, TL—tribo layers).

(**a**) (**b**)

Figure 6. COF curve of IPS e.max CAD under polished surface (in the presence of artificial saliva and 10,000 fretting cycles): (**a**) 250 mN, 4 mm/s; (**b**) 1000 mN, 12 mm/s.

3.3. Optimization of ANN Hyperparameters Using Genetic Algorithm

In this section, the results obtained from the application of a GA for optimizing the hyperparameters of ANNs trained on three types of processed lithium disilicate surfaces, polished, glazed, and ground, are presented. The optimization process was aimed at enhancing the prediction accuracy for the wear rate and coefficient of friction, which were influenced by varying parameters such as normal force and sliding velocity.

The GA was applied to fine-tune the hyperparameters of the ANNs, which were trained on data obtained from tribological testing of the three types of surfaces. The optimization and training processes were conducted for each surface type, with specific time intervals for each process. Each training procedure lasted 50 generations, with a population size of 20 members per generation. The time durations for optimization and training were as follows: 1611.33 s for the polished surface, 1487.46 s for the glazed surface, and 1352.44 s for the ground surface. Figure 7 illustrates the progression of the mean squared error (MSE) values across iterations, highlighting the best and average values within each population.

The graphs illustrate the convergence of the GA over 50 generations, depicting the penalty values for the best individual (black dots) and the mean penalty values across the entire population (blue dots) for each generation. The penalty values demonstrate a rapid decrease during the initial 10 generations for all three cases, indicating an efficient exploration of the solution space. Beyond the 15th generation, the penalty values stabilize, signaling the algorithm's convergence toward an optimal solution. The best-achieved penalty MSE values are 0.000554227, 0.000279777, and 7.29834×10^5 for the polished, glazed, and ground surface, respectively, while the mean MSE penalty value in the final generation is 0.00118152, 0.00330609, and 0.00539462 for the polished, glazed and ground surface, respectively. This discrepancy highlights the algorithm's capability to identify superior solutions within the population. The stabilization of the mean MSE penalty value across later generations confirms the population's adaptation to optimal regions of the search space. This observation underscores the robustness of the GA in solving complex optimization problems. The results validate the effectiveness of the implemented GA in minimizing the MSE penalty function. The rapid convergence and the achieved optimal penalty value reflect the algorithm's ability to optimize model parameters efficiently while maintaining population diversity during the initial stages of evolution.

Table 5 presents the selected hyperparameters for the ANN models corresponding to the three types of processed lithium disilicate surfaces: polished, glazed, and ground.

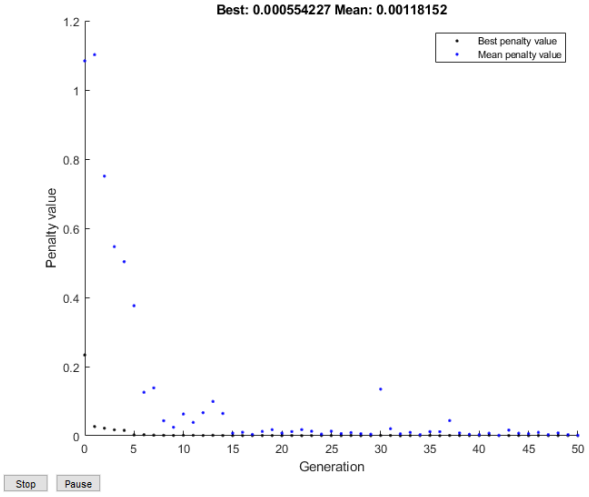

(**a**) Polished surface

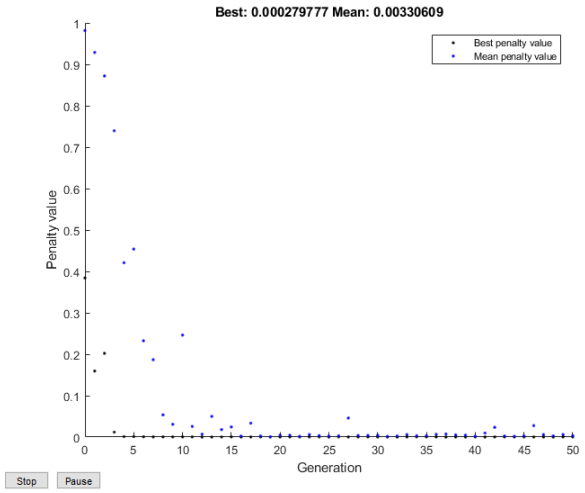

(**b**) Glazed Surface

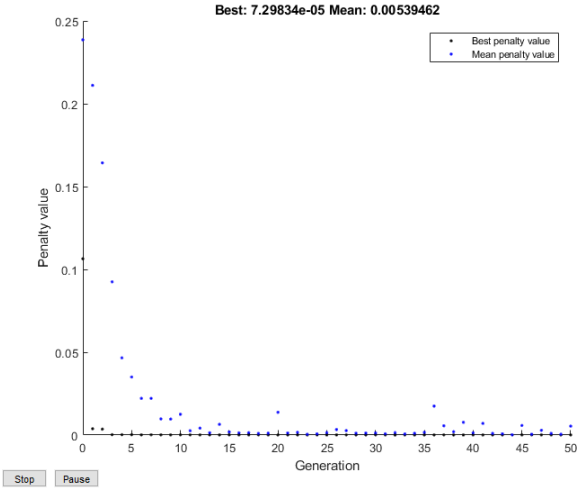

(**c**) Ground Surface

Figure 7. MSE through optimization processes for different surface types: (**a**) polished surface; (**b**) glazed surface; (**c**) ground surface.

Table 5. Summary of ANN best models hyperparameters.

Hyperparameter	Polished Surface	Glazed Surface	Ground Surface
Number of hidden neurons	17	21	20
Transfer function for hidden layer	Softmax Transfer Function	Softmax Transfer Function	Logarithmic Sigmoid Transfer Function
Transfer function for output layer	Elliott Sigmoid Transfer Function	Elliott Sigmoid Transfer Function	Elliott Sigmoid Transfer Function
Training validation test ratio	0.97428/ 0.012859/ 0.012859	0.96174/ 0.019132/ 0.019132	0.95128/ 0.024359/ 0.024359
Number of epochs	1000	1000	1000
Training function	Levenberg–Marquardt Backpropagation	Levenberg–Marquardt Backpropagation	Levenberg–Marquardt Backpropagation

The hyperparameter configurations for the ANN models corresponding to the polished, glazed, and ground surfaces of lithium disilicate material, as presented in Table 5, reveal several critical insights regarding the model architecture and training strategies employed.

The number of hidden neurons varies slightly among the surfaces, reflecting differences in the data complexity for each type. The polished surface model, with 17 hidden

neurons, indicates a simpler architecture, suggesting that the patterns in the data for this surface are relatively less complex. Conversely, the glazed surface model employs 21 hidden neurons, implying a more intricate structure to accommodate the potentially higher variability or complexity in its data. The ground surface model, with 20 hidden neurons, represents an intermediate level of complexity, tailored to balance simplicity and effectiveness for this surface type.

Regarding the transfer function for the hidden layer, the polished and glazed surface models utilize the Softmax Transfer Function. This choice is often associated with tasks involving multi-class classification or when the network outputs probabilistic distributions. In contrast, the ground surface model adopts the Logarithmic Sigmoid Transfer Function, which is well suited for regression tasks and ensures smoother activations with outputs constrained within a specific range (0 to 1). These distinctions indicate that the activation function was selected to match the expected characteristics of the output data for each surface type.

All three models share a common transfer function for the output layer, the Elliott Sigmoid Transfer Function. This function is particularly effective in regression problems, enabling predictions to be scaled within a bounded range, which aligns with tasks requiring precise numerical outputs, such as the minimization of the MSE.

The training validation test ratios exhibit slight variations among the surfaces. The polished surface model dedicates 97.428% of the data to training, with only 1.2859% allocated to both validation and testing, emphasizing a focus on model accuracy through extensive training data. The glazed surface model uses a slightly lower training proportion (96.174%) while retaining a comparable split for validation and testing. The ground surface model allocates 95.128% to training, with a relatively larger share (2.4359%) devoted to validation and testing. This increased allocation to validation and testing suggests a greater emphasis on model generalization for the more complex ground surface data.

Each model was trained for 1000 epochs, ensuring sufficient iterations for optimizing the network's weights and achieving convergence. This uniform choice across all surface types reflects a consistent training strategy designed to fully leverage the available data.

Finally, the models employed the Levenberg–Marquardt backpropagation algorithm for training. This algorithm is renowned for its efficiency and stability, especially with small- to medium-sized datasets, as it combines the advantages of the Gauss–Newton method and gradient descent. Its application underscores a deliberate choice to accelerate convergence while maintaining a robust performance across all models.

In summary, the ANN models for the polished, glazed, and ground surfaces demonstrate a thoughtful design and tuning of hyperparameters tailored to the specific data characteristics of each surface type. Variations in the number of hidden neurons and the transfer functions reflect the differing complexities of the data, while consistent training strategies, including the allocation of epochs and the choice of the Levenberg–Marquardt algorithm, underscore a well-structured approach to optimizing model performance for each case.

3.4. Visual Representation and Comparison of Wear and Friction Predictions

After selecting the best ANN models using a GA, these models were employed for the visual representation and comparison of real wear and friction values with the predicted wear and friction values. Figures 8–10 present the surface plots depicting the wear and friction values for force intervals ranging from 0 to 1 N and velocity intervals spanning from 4 to 12 mm/s. These visualizations offer a comprehensive representation of the variation in wear and friction across the three surface types—polished, glazed, and ground—highlighting the distinct characteristics of each surface. The surface plots illustrate the predicted and known values of wear (left plots) and friction (right plots) under varying

conditions of velocity and normal force. In each figure, the predicted values are represented as continuous surfaces while the known values are marked with red points, providing a comparative visualization of model performance.

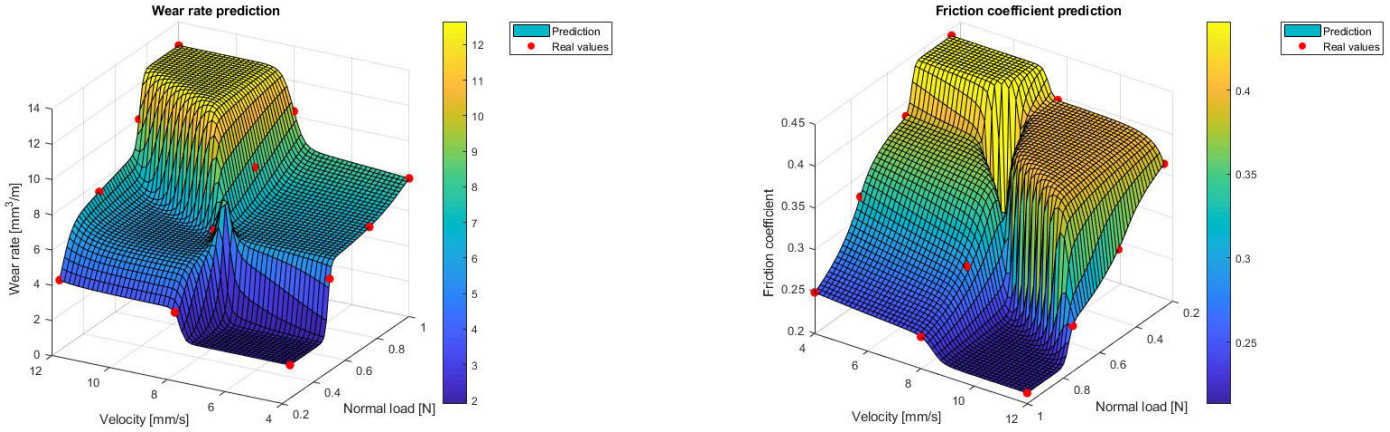

Figure 8. Polished surface—predicted wear rate and friction coefficient by ANN models using a GA vs. real values of wear rate and friction coefficient.

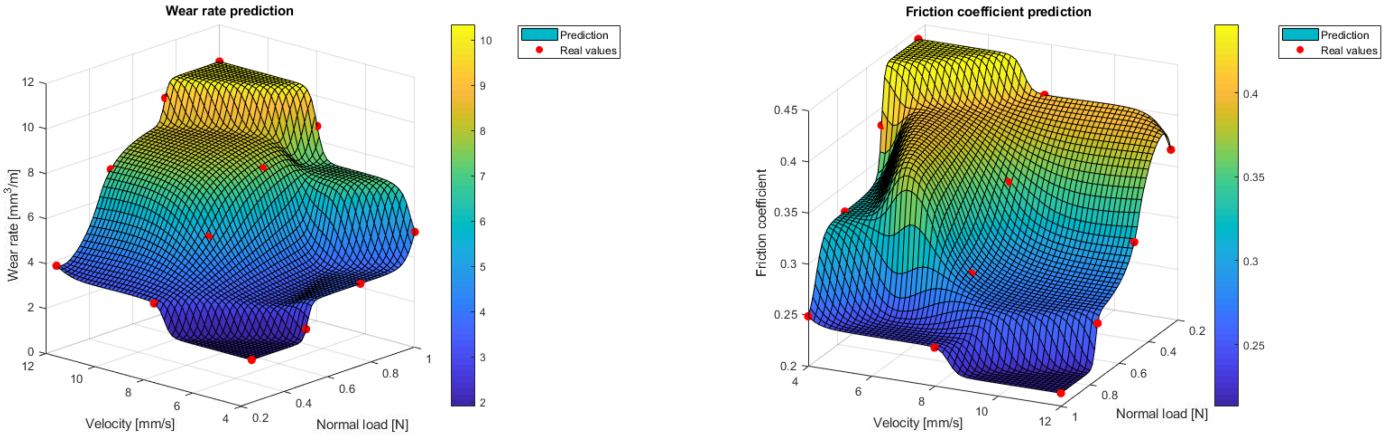

Figure 9. Glazed surface—predicted wear rate and friction coefficient by ANN models using a GA vs. real values of wear rate and friction coefficient.

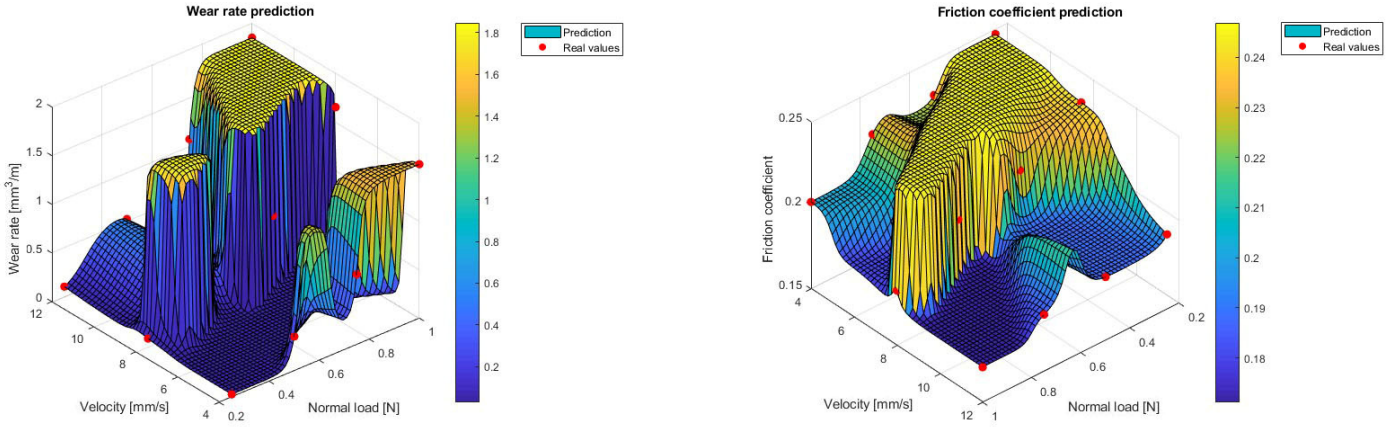

Figure 10. Ground surface—predicted wear rate and friction coefficient by ANN models using a GA vs. real values of wear rate and friction coefficient.

For the wear rates prediction plots (positioned left in Figures 8 and 9), the surface exhibits nonlinear behavior, with wear values increasing significantly as the normal force approaches its upper limit (near 1) and velocity increases. The red points align closely with

the predicted surface, highlighting the model's accuracy in capturing the observed data. This suggests that wear rates are more pronounced under higher normal loads and velocity conditions for both finishing techniques (polished and glazed), with a maximal value of 14 mm^3/m. In the COF prediction plot (positioned right in Figures 8 and 9), the COF values also demonstrate nonlinear behavior, with variations dependent on the interplay between normal load and velocity. The COF values decrease with increasing velocity and normal force but plateau at higher levels, indicating a potential stabilization of friction under specific conditions. What is characteristic of these processed surfaces is that the maximum coefficient of friction is approximately 0.44 and occurs at the lowest sliding velocity and the smallest applied force. The predictions shown in Figures 8 and 9 are fully consistent with the obtained values of the experimental tribological results.

In the wear rate prediction plot (positioned left in Figure 10), the surface exhibits significant variability with sharp transitions, reflecting the nonlinear relationship between wear rate, velocity, and normal load. Wear rate values generally increase with velocity and normal force, with notable peaks in specific regions, indicating heightened wear sensitivity under certain conditions. The red points align well with the surface, particularly in critical regions, showcasing the model's ability to capture complex patterns effectively. Compared to the previous two surfaces, the wear rate trend of the ground surface is more gradual. Depending on the sliding velocity, the increase in wear remains within a narrow range for all values of normal load, which is corroborated by the obtained experimental results. The COF prediction plot (positioned right in Figure 10) illustrates a smoother surface compared to the wear prediction but still captures subtle variations influenced by the input parameters. The COF values decrease gradually with normal force and velocity, stabilizing in specific ranges. The close proximity of red markers to the surface highlights the model's precision in approximating observed friction values. The lowest coefficient of friction under various testing conditions, which include variations in three sliding velocities and four load levels, is observed for the ground surface, which is confirmed by the experimental findings.

Overall, these surface plots validate the model's ability to capture complex relationships between velocity, normal load, and the resulting wear rate and friction coefficient. The alignment of the red markers with the surface further validates the model's predictive reliability. The close correspondence between predicted and known values indicates the robustness and accuracy of the developed ANN model for polished and glazed surfaces.

In summary, for wear prediction, the surfaces consistently exhibit nonlinear behavior, with wear values increasing significantly as normal force and velocity rise. Notable increases in wear occur when normal force approaches its upper limit and velocity increases, indicating that higher forces and velocities contribute to material wear. The red points closely align with the predicted surfaces in most regions, confirming the model's accuracy in capturing the observed data. In the friction prediction plots, a nonlinear relationship is also observed. Friction values decrease with velocity and normal force increase, but they plateau at higher levels, suggesting that friction stabilizes under certain conditions. Subtle variations in the surface gradient reflect complex interactions between the parameters, and the red markers' alignment with the surface further validates the model's predictive reliability. Across all figures, the close correspondence between the predicted and known values demonstrates the robustness and accuracy of the ANN model. These visualizations highlight the model's ability to handle intricate interactions between velocity, normal force, and the resulting wear and friction, underscoring the effectiveness of the optimization and training processes used in its development.

4. Discussion

Accurately predicting wear rate and friction coefficient behavior in dental ceramics remains a critical challenge due to the complex interplay of mechanical loading, material microstructure, and surface treatments, necessitating advanced computational approaches to enhance predictive accuracy and material optimization. The findings of this study demonstrate that the application of genetic algorithm (GA) optimization significantly enhances the predictive accuracy of artificial neural networks (ANNs) for wear and friction estimation across different surface treatments of lithium disilicate, as evidenced by a reduced mean squared error (MSE) and strong correlations between actual and predicted values, as confirmed by Figures 8–10.

In comparison to previous studies, our research relies on the application of a GA for fine-tuning ANN parameters in tribological testing, which significantly improved the model accuracy. Earlier studies did not use optimization techniques that could handle the complexities of tribological data, such as variations in normal force and sliding velocity, which often leads to overfitting and reduced generalization. Our application of the GA not only improved the performance in terms of reducing the MSE but also enabled the selection of relevant hyperparameters, further enhancing the model's robustness.

Additionally, it is important to note how the results of this study fit into the broader context of research in tribology and dental material processing. Specifically, the increased accuracy in predicting wear and friction behavior enables better understanding and optimization of operational conditions for materials such as lithium disilicate. Our results suggest that parameters such as velocity and normal force are critical for prediction accuracy in tribological testing, aligning with previous research that showed similar findings regarding the interaction between these factors and material performance.

While this study demonstrates the effectiveness of ANN models optimized using a genetic algorithm (GA) for predicting wear and friction in lithium disilicate ceramics, several limitations should be acknowledged. First, the dataset used for model training and validation is limited to specific experimental conditions, including predefined sliding velocities and normal loads. As a result, the generalization of the model to a wider range of operational conditions, such as varying humidity, temperature, or different lubrication environments, remains uncertain. Additionally, the study primarily focuses on three surface treatment methods—polished, glazed, and ground—without considering other clinically relevant finishing techniques or potential variations in surface roughness that may influence tribological behavior. Future research should explore additional surface treatments and include topographical analyses to enhance predictive accuracy.

Finally, it is important to note that future studies should explore how different surface treatments affect long-term material performance in order to develop optimized strategies for longer lifespan and cost reduction in industrial applications. While our results are promising, additional research may contribute to further optimization and increase the applicability of this methodology to a wider range of tribological tests.

5. Conclusions

This study highlights the potential of ANNs as a valuable tool for predicting and optimizing the tribological properties of dental glass ceramics, specifically lithium disilicate (Li_2SiO_3). By combining experimental data with advanced computational techniques, such as hyperparameter optimization through a GA, this study successfully demonstrated the capacity of ANNs to model the complex, nonlinear relationships between material properties, environmental conditions, and operational parameters. The results confirmed that ANNs can effectively predict wear and friction behaviors, which are essential for understanding the performance and longevity of dental materials under various conditions.

The findings also underscore the significance of a surface finish on the tribological performance of lithium disilicate, with distinct differences observed between polished, glazed, and ground surfaces. The tribological tests conducted in artificial saliva, simulating realistic oral conditions, revealed that the wear and friction coefficients vary considerably depending on the surface treatment, providing valuable insights into the material's performance in practical applications.

Moreover, this research contributes to the growing body of literature on the application of ML in material science, particularly in the optimization of dental glass ceramics. It bridges the gap between traditional experimental methods and modern computational tools, offering a more efficient and scalable approach to material development. By reducing the reliance on exhaustive experimental testing, ANN-based models can accelerate the design process and lead to the creation of enhanced materials with superior tribological properties.

In conclusion, this study demonstrates that integrating ANNs with experimental data presents a powerful approach for the prediction and optimization of tribological properties, offering significant potential for advancing material science and engineering, particularly in the field of dental materials. This research shows the way for future studies that explore the broader applications of ML in material optimization, potentially revolutionizing the development of high-performance materials for various industries.

Author Contributions: Conceptualization, M.P. and A.D.; methodology, M.P.; software, S.P.S.; validation, S.J., Ž.Š. and M.R.; formal analysis, M.R.; investigation, S.J.; resources, M.P.; data curation, A.D.; writing—original draft preparation, S.P.S.; writing—review and editing, Ž.Š.; visualization, S.J.; supervision, Ž.Š.; project administration, M.R.; funding acquisition, M.R, S.J. and Ž.Š. All authors have read and agreed to the published version of the manuscript.

Funding: This research received no external funding.

Informed Consent Statement: Not applicable.

Data Availability Statement: The original contributions presented in the study are included in the article, further inquiries can be directed to the corresponding author.

Conflicts of Interest: The authors declare no conflicts of interest.

References

1. Hutchings, I.M.; Shipway, P. *Tribology: Friction and Wear of Engineering Materials*; Butterworth-Heinemann: Oxford, UK, 2017.
2. Bhushan, B. *Principles and Applications of Tribology*; John Wiley & Sons: Hoboken, NJ, USA, 2013.
3. Stachowiak, G.W.; Batchelor, A.W. *Engineering Tribology*; Butterworth-Heinemann: Oxford, UK, 2013.
4. Pantić, M. Tribological Characterization of Advanced Dental Materials. Ph.D. Thesis, Faculty of Engineering, University of Kragujevac, Kragujevac, Serbia, 2017.
5. Babic, M.; Stojanovic, B.; Dzunic, D.; Pantic, M. Micro/nanoscale structural, mechanical and tribological characterization of ZA-27/SiC nanocomposites. *J. Compos. Mater.* **2020**, *54*, 2113–2129. [CrossRef]
6. Zhang, Z.; Friedrich, K.; Velten, K. Prediction on tribological properties of short fibre composites using artificial neural networks. *Wear* **2002**, *252*, 668–675. [CrossRef]
7. Yetim, A.; Codur, M.; Yazici, M. Using of artificial neural network for the prediction of tribological properties of plasma nitrided 316L stainless steel. *Mater. Lett.* **2015**, *158*, 170–173. [CrossRef]
8. Suryawanshi, A.; Behera, N. Prediction of wear of dental composite materials using machine learning algorithms. *Comput. Methods Biomech. Biomed. Eng.* **2024**, *27*, 400–410. [CrossRef] [PubMed]
9. LiuJie, X.; Davim, J.; Cardoso, R. Prediction on tribological behaviour of composite PEEK-CF30 using artificial neural networks. *J. Mater. Process. Technol.* **2007**, *189*, 374–378. [CrossRef]
10. Gyurova, L.; Friedrich, K. Artificial neural networks for predicting sliding friction and wear properties of polyphenylene sulfide composites. *Tribol. Int.* **2011**, *44*, 603–609. [CrossRef]
11. Jia, B.; Wan, Q.; Yan, L.; Luo, Y.; Wei, Q.; Niu, C.; Yang, B.; Li, S.; Meng, L. Tribological properties and machine learning prediction of FeCoCrNiAlN high entropy coatings. *Surf. Coat. Technol.* **2024**, *477*, 130341. [CrossRef]

12. Wang, R.; Hass, V.; Wang, Y. Machine learning analysis of microtensile bond strength of dental adhesives. *J. Dent. Res.* **2023**, *102*, 1022–1030. [CrossRef] [PubMed]
13. Suryawanshi, A.; Behera, N. Prediction of abrasive wears behavior of dental composites using an artificial neural network. *Comput. Methods Biomech. Biomed. Eng.* **2023**, *26*, 710–720. [CrossRef] [PubMed]
14. Kelly, J.R.; Benetti, P. Ceramic materials in dentistry: Historical evolution and current practice. *Aust. Dent. J.* **2011**, *56*, 84–96. [CrossRef]
15. Zhang, Y.; Lawn, B.R. Novel zirconia materials in dentistry. *J. Dent. Res.* **2018**, *97*, 140–147. [CrossRef] [PubMed]
16. Derchi, G.; Marchio, V.; Cinquini, C.; Federici, M.I.; Barone, A.; Pagano, S. Evaluation of Accuracy of Different Print Angulations for 3D Printed Dental Crowns. *Medziagotyra* **2024**, *30*, 114–120. [CrossRef]
17. Denry, I.; Holloway, J.A. Ceramics for dental applications: A review. *Materials* **2014**, *3*, 351–368. [CrossRef]
18. Fischer, K.; Bühler-Zemp, P.; Völkel, T. *Scientific Documentation IPS e.max Cad*; Ivoclar-Vivadent AG: Schaan, Liechtenstein, 2011.
19. Lawson, N.C.; Janyavula, S.; Syklawer, S.; McLaren, E.A.; Burgess, J.O. Wear of enamel opposing zirconia and lithium disilicate after adjustment, polishing and glazing. *J. Dent.* **2014**, *42*, 1586–1591. [CrossRef] [PubMed]
20. Available online: https://www.medin.cz/media/cache/file/39/MEDIN_Catalogue_rotary_instruments_for_dentistry_2020-04.pdf (accessed on 3 February 2025).
21. Mukherjee, S. *Applied Mineralogy*, 1st ed.; Springer: Dordrecht, The Netherlands, 2011; pp. 1–196.
22. Zhou, Z.; Zheng, J. Oral tribology. *Proc. Inst. Mech. Eng. Part J J. Eng. Tribol.* **2006**, *220*, 739–754. [CrossRef]
23. Hahn Berg, I.; Rutland, M.; Arnebrant, T. Lubricating properties of the initial salivary pellicle—An AFM study. *Biofouling* **2003**, *19*, 365–369. [CrossRef]
24. Sharma, S.; Sangal, S.; Mondal, K. On the optical microscopic method for the determination of ball-on-flat surface linearly reciprocating sliding wear volume. *Wear* **2013**, *300*, 82–89. [CrossRef]
25. Available online: https://cdn.standards.iteh.ai/samples/94690/8ffde8b28de642f192d4971c9e3f5e8f/ASTM-G133-05-2016-.pdf (accessed on 3 February 2025).
26. Hutchings, I.M. *Tribology: Friction and Wear of Engineering Materials*, 1st ed.; Edward Arnold Publishers Ltd.: Ann Arbor, MI, USA, 1992.